ACS APPLIED MATERIALS & INTERFACES

Research Article

www.acsami.org

Epigallocatechin-3-gallate (EGCG)-Stabilized Selenium Nanoparticles Coated with Tet-1 Peptide To Reduce Amyloid-β Aggregation and Cytotoxicity

Jingnan Zhang,[†] Xianbo Zhou,[†] Qianqian Yu, Licong Yang, Dongdong Sun, Yanhui Zhou, and Jie Liu*

Department of Chemistry, Jinan University, Guangzhou 510632, China

Supporting Information

ABSTRACT: Alzheimer's disease (AD), the most common neurodegenerative disease, is caused by an accumulation of amyloid-β (Aβ) plaque deposits in the brains. Evidence is increasingly showing that epigallocatechin-3-gallate (EGCG) can partly protect cells from Aβ-mediated neurotoxicity by inhibiting Aβ aggregation. In order to better understand the process of Aβ aggregation and amyloid fibril disaggregation and reduce the cytotoxicity of EGCG at high doses, we attached EGCG onto the surface of selenium nanoparticles (EGCG@Se). Given the low delivery efficiency of EGCG@Se to the targeted cells and the involvement of selenoprotein in antioxidation and neuroprotection, which are the key factors for preventing the onset and progression of AD, we synthesized EGCG-stabilized selenium nanoparticles coated with Tet-1 peptide (Tet-1-EGCG@Se, a synthetic selenoprotein analogue), considering the affinity of Tet-1 peptide to neurons. We revealed that Tet-1-EGCG@Se can effectively inhibit Aβ fibrillation and disaggregate preformed Aβ fibrils into nontoxic aggregates. In addition, we found that both EGCG@Se and Tet-1-EGCG@Se can label Aβ fibrils with a high affinity, and Tet-1 peptides can significantly enhance the cellular uptake of Tet-1-EGCG@Se in PC12 cells rather than in NIH/3T3 cells.

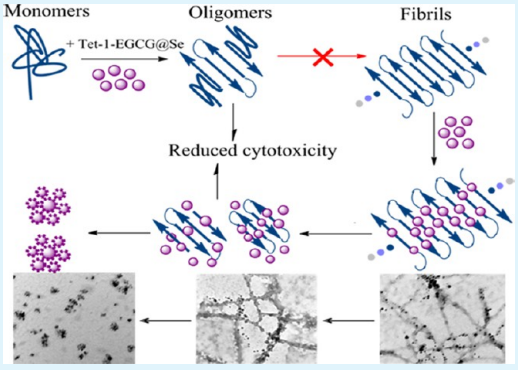

KEYWORDS: *selenium nanoparticles, epigallocatechin-3-gallate, amyloid, oligomer, fibril*

1. INTRODUCTION

Alzheimer's disease (AD) is the most common form of dementia and a growing concern in the modern world.[1] Nowadays the number of individuals affected with AD is increasing exponentially.[2−4] Therefore, strategies for AD therapy are among the most challenging and timely areas of study in modern medicine. AD pathology in the brain concludes amyloid plaque accumulation, τ protein hyperphosphorylation, oxidative stress, and cell apoptosis.[5−10] However, the molecular mechanisms of AD pathogenesis are not fully understood.[11] Recent studies have demonstrated that amyloid-β (Aβ) polymerization may be crucial to AD pathologies.[2] Therefore, there has been considerable effort to develop new drugs that inhibit Aβ fibrillation.

Epigallocatechin-3-gallate (EGCG), the major polyphenol in green tea, is known for its potent antioxidant properties and has recently attracted interest because of its emerging biological activities.[12−14] Previous reports suggest that EGCG interacts with a large variety of amyloid-forming proteins such as Aβ,[15] α-synuclein,[16] transthyretin,[17] and huntingtin,[18] which are involved in neurodegeneration. Importantly, EGCG can redirect the amyloid formation pathways of Aβ and partly promote the assembly of low-toxicity aggregate structures.[19−22] It is suggested that EGCG is a promising new drug-delivery system to the special position.[23,24] However, the efficiency of targeted cellular uptake and bioavailability of EGCG are quite low, which is mainly attributed to its poor stability and polyhydroxy structure.[25] In addition, EGCG causes cytotoxicity at high concentration.[23,26] Considering these limitations, we synthesized the nanostructured biomaterials of EGCG to improve EGCG potential therapeutic efficacy.

Selenium (Se) is an essential trace element nutritionally important to mammals, and it can assist cells to resist oxidative damage. In vivo, Se is primarily present as various selenoproteins, which play important roles in cellular redox regulation, detoxification, and immune-system protection.[27] So far, 25 selenoproteins have been found in humans and 24 in rodents.[28] Recently, high interest has been focused on the role of Se and selenoproteins in neurodegenerative diseases such as AD. Selenoprotein is highly expressed in the human brain and most likely involved in antioxidation and neuroprotection, which are the major factors for preventing the onset and progression of AD.[29] However, the chemical and biological functions of some newly synthesized selenoprotein analogues remain unknown.[30] In this context, the aim of this study was to

Received: March 6, 2014
Accepted: April 23, 2014
Published: April 23, 2014

   dx.doi.org/10.1021/am501341u | ACS Appl. Mater. Interfaces 2014, 6, 8475−8487

investigate the potential neuroprotective effects of Se nanoparticles (NPs).

Firstly, we synthesized EGCG-stabilized SeNPs (EGCG@Se). Then we synthesized EGCG@Se coated with Tet-1 peptide (Tet-1-EGCG@Se) considering the following advantages of Tet-1 peptide: Tet-1, a 12-amino acid peptide that has the binding characteristics of tetanus toxin, was identified by Boulis and workers through phage display.[31,32] It can interact specifically with neurons with the capability of retrograde delivery in the neuronal cells. The amino acid sequence of Tet-1 peptide is "HLNILSTLWKYR",[31−33] identified by Liu et al.

Here, we reported on the interactions between Tet-1-EGCG@Se and Aβ. To compare the specificity of Aβ fibril affinity, citric acid stabilized SeNPs (CA@Se) have been used here. We further investigated the cellular uptake of Tet-1-EGCG@Se in PC12 cells by inductively coupled plasma atomic emission spectrometry (ICP-AES) analysis. Our results reveal that the selenoprotein analogue Tet-1-EGCG@Se can label the Aβ fibrils with a high affinity, inhibit Aβ fibrillation, disaggregate preformed Aβ fibrils, and also target PC12 cells.

2. EXPERIMENTAL SECTION

2.1. Materials and Reagents. Sodium selenite (Na_2SeO_3) was purchased from Sigma-Aldrich Chemical Co. Amyloid-β ($A\beta_{1\text{-}40}$) and Tet-1 peptides (HLNILSTLWKYR) were synthesized by solid-phase Fmoc chemistry at GL Biochem Ltd. (Shanghai, China). The final sample was verified by electrospray ionization mass spectrometry. 2′,7′-Dichlorodihydrofluorescein diacetate (DCFH-DA), bicinchoninic acid (BCA) kit for protein determination, and epigallocatechin-3-gallate (EGCG; 98% purity) were purchased from Sigma. A terminal transferase dUTP nick end labeling (TUNEL) assay kit was obtained from Roche Applied Science (Basel, Switzerland). Fetal bovine serum (FBS) and horse serum were purchased from Gibco (Life Technologies AG, Zug, Switzerland). Dulbecco modified Eagle's medium (DMEM) was purchased from Invitrogen Corp. 3-(4,5-Dimethylthiazol-2-yl)-2,5-diphenyltetrazolium bromide (MTT), 4′,6-diamidino-2-phenylindole (DAPI), and thioflavine T (ThT) were from Sigma (St. Louis, MO). All reagents and solvents were purchased commercially and used without further purification unless specially noted.

Peptides were prepared as indicated in the literature.[34−36] Briefly, powdered Aβ was first dissolved in 1,1,1,3,3,3-hexafluoro-2-propanol (HFIP) at a concentration of 1 mg mL^{-1}. The solution was shaken at 4 °C for 2 h in a sealed vial for further dissolution and was then stored at −20 °C as a stock solution. Before use, the solvent HFIP was removed by evaporation under a gentle stream of nitrogen, and the peptide was prepared by dissolving Aβ (0.5 mM) in phosphate-buffered saline (PBS; 10 mM, pH 7.4) and sonicating it for 1 min in a water bath. This solution was diluted with water (500 μL), sonicated for 1 min, adjusted to pH 7.4 using NaOH (0.5 M) and HCl (0.5 M), and then filtered through a 0.22 μm filter (Millipore). Aβ-related experiments were performed at least in triplicate with the discrepancy between individual values less than 5%.

2.2. Preparation of EGCG@Se and the Coating of Tet-1 Peptides. EGCG@Se was prepared as follows. Six NP formulations were prepared for the study with various ratios of EGCG to Na_2SeO_3. Formulations prepared for this study were 10:1, 8:1, 6:1, 4:1, 2:1, and 1:1 (EGCG to Na_2SeO_3 on a molar basis). Na_2SeO_3 was first solubilized in a water-in-ethanol solution (step 1). Anhydrous EGCG was added to the materials in step 1 and cosolubilized by mixing at room temperature (step 2). EGCG@Se was produced by adding distilled water while materials were mixed for 2 h (step 3).

For the coating of Tet-1 peptides with EGCG@Se, the cosolubilization methodology and electrostatic bonding effect were employed in the latter experiment. Briefly, the synthesized EGCG@Se was dissolved with Milli-Q water at a suitable concentration, and then an aqueous solution of Tet-1 peptides was added to the solution slowly with stirring at room temperature for 4 h (pH 5.0). Then, the homogeneous solution was centrifuged at 20000 rpm for 20 min to obtain the specific NP. After the supernatant was decanted, the precipitates were washed 10 times with Milli-Q water.

2.3. Characterization of NPs. The as-prepared products were characterized by using microscopic and spectroscopic methods. In brief, the ζ potential and size distribution of the NPs were measured by a Nano-ZS instrument. Transmission electron microscopy (TEM) samples were prepared by dispersing the NP solutions (10 μL) onto a holey carbon film on copper grids and washed with deionized water, dried under IR light. The micrographs were obtained on a Hitachi instrument for TEM operated at an accelerating voltage of 80 kV. NP solutions for atomic force microscopy (AFM) were deposited onto freshly cleaved mica and incubated at room temperature for 3 min. The remaining salts and loose deposits in the suspension were subsequently rinsed with ultrapure water and then dried with N_2. AFM images were obtained on a Nanoscope V Multimode scanning probe workstation using etched silicon Nano-Probes under ambient conditions. AFM analysis was carried out in tapping mode, and images were acquired at a resolution of 512 × 512 pixels. A diode-array spectrophotometer was used for characterization of the effects of Tet-1 peptide with EGCG@Se at a 240−800 nm wavelength range using a 1 cm quartz cuvette. Fourier transform infrared spectroscopy (FT-IR) spectra of the samples were recorded on an Equinox 55 IR spectrometer in the range of 4000−400 cm^{-1} using the KBr-disk method. Scanning electron microscopy−energy-dispersive X-ray (SEM−EDX) analysis was carried out on an EX-250 system (Horiba) and employed to examine the elemental composition of the NPs.

2.4. Adsorption Efficiency of Tet-1 Peptide to EGCG@Se. Adsorption efficiency of Tet-1 peptide to EGCG@Se was quantified by measuring the absorbance intensity of the centrifuged NPs using a trace BCA kit. The concentration of EGCG@Se was kept constant (2 mg mL^{-1}). The amount of peptide coating EGCG@Se was calculated from the absorbance intensity of a known amount of peptide dissolved in PBS.

2.5. ThT Fluorescence Assessment. The kinetics of Aβ aggregation was monitored by using the dye ThT, the fluorescence of which is dependent on the formation of amyloid fibrils. Aβ was coincubated with different NPs in PBS buffer with 100 rpm agitation for 48 h at 37 °C. At different times, aliquots of the Aβ solution were taken for fluorescence measurements. Fluorescence measurements were carried out with a spectrofluorometer. The fluorescence signal was recorded at 480 nm; 10 nm slits were used for both emission and excitation measurements. The Aβ concentration was 20 μM, and the ThT concentration was 10 μM.

2.6. Measurement of Soluble Aβ. Aβ aggregation was further studied by measuring the percentage of soluble Aβ in the supernatant of the reaction mixtures. Aβ was coincubated with different NPs in PBS buffer with 100 rpm agitation for 48 h at 37 °C. The soluble Aβ concentration was determined with BCA protein assay after centrifugation at 20000 rpm for 20 min (both NPs and aggregated Aβ were precipitated).

2.7. Sodium Dodecyl Sulfate Polyacrylamide Gel Electrophoresis (SDS-PAGE). Aliquots of each reaction mixture prepared for ThT fluorescence assay were separated by electrophoresis at 40 mV for 1 h at room temperature using 15% SDS−polyacrylamide gels. SDS and β-mercaptoethanol were present in both running and sample buffers, but the samples were not preheated. The gels were stained following a silver stain protocol.

2.8. TEM. Negative-staining TEM samples were prepared as follows. A 10 μL volume of sample prepared for ThT fluorescence assessment was applied to a formvar/carbon-coated grid for 2 min and blotted with filter paper. The sample was stained with a 2% uranyl acetate aqueous solution for 2 min and blotted. Finally, the grids were washed twice with filtered (0.2 μm) water and air-dried. Images were obtained using a Hitachi (H-7650) transmission electron microscope operating at 80 kV. Intensity measurements between replicates typically deviate less than 10%.

2.9. AFM Studies. Solutions prepared for ThT fluorescence assessment were deposited onto freshly cleaved mica (Φ 1 cm) and

Scheme 1. Plan for the Synthesis of Tet-1-EGCG@Se

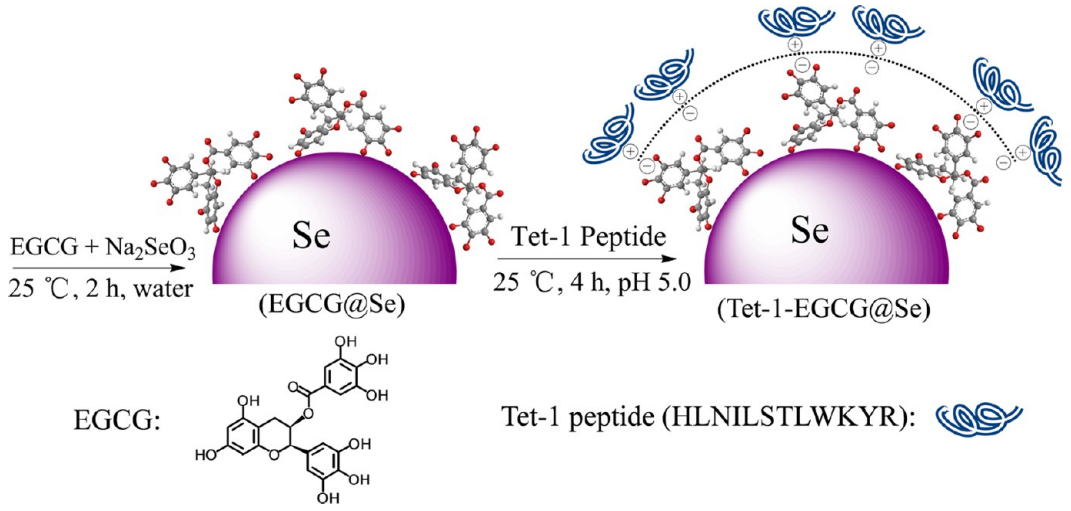

incubated at room temperature for 3 min. The remaining salts and loose deposits in the suspension were subsequently rinsed with ultrapure water (50 μL, Millipore) and then dried with N_2. AFM images were obtained on a Nanoscope V Multimode scanning probe workstation using etched silicon Nano-Probes under ambient conditions. At least three different regions of the surface were examined to verify that morphology was similar throughout the sample. The images were analyzed by using the Nanoscope V software from the AFM supplier. The results presented show both height and amplitude images.

2.10. Fibril Disaggregation Assay. For the Aβ fibril disaggregation assay, the Aβ solution was preincubated at 37 °C, followed by 100 rpm agitation for 3 days to obtain the sufficient amyloid fibrils. Kinetic studies with ThT and circular dichroism (CD) clearly indicated that these conditions enable one to reach the maximal level of aggregation. EGCG, EGCG@Se, or Tet-1-EGCG@Se was added into the preformed Aβ fibril solutions for further incubation. During and after 6−72 h of incubation, samples were examined by TEM and AFM. To check the specificity of the NPs, CA@Se (10 μg mL^{-1}) was added to Aβ fibril solutions and incubated further for 6 and 12 h. The final reaction mixture was analyzed by TEM as mentioned above.

2.11. Investigation of the Conformation by CD. Final solutions from fibril disaggregation assay were directly applied with CD. CD spectra of the samples in the range of 190−290 nm were recorded on a JASCO J-810 automatic recording spectropolarimeter (Tokyo, Japan) controlled by the Jasco software. The data of the baseline acquired in the absence of Aβ were subtracted from each spectrum.

2.12. Cytotoxicity Assays. PC12 cells originally obtained from American Tissue Type Cell Collection were grown in DMEM supplemented with 5% horse serum, 10% FBS, and 1% antibiotics (penicillin/streptomycin) at 37 °C in a humidified 95% air/5% CO_2 incubator. Cells were treated with solutions from ThT fluorescence assessment and fibril disaggregation assay in a freshly prepared serum-free neurobasal medium for 48 h. Controls were only treated with the vehicle or with inhibitors. The cell viability was tested by measuring formazan produced by the reduction of MTT.

2.13. Measurement of the Intracellular Reactive Oxygen Species (ROS) Level. Free-radical production was measured by incubating the cells with the fluorescent probe (DCFH-DA; Molecular Probe, Sigma). The DCFH-DA dye was used to measure the relative levels of cellular peroxides.[9,37] PC12 cells were treated with disaggregated Aβ fibril in the presence or absence of EGCG, EGCG@Se, or Tet-1-EGCG@Se within a serum-free medium and then incubated at 37 °C for 24 h. After incubation, cells were treated with 5 μM DCFH-DA for 30 min at 37 °C. Cells were then washed once with a standard medium before measurement. Fluorescence was measured at 488 nm excitation and 530 nm emission wavelengths by a FACS Calibur (BD Biosciences).

2.14. TUNEL−DAPI Staining Assay. Protection against DNA fragmentation induced by Aβ was testified by using an in situ cell death detection kit following the manufacturer's protocol. In short, cells were treated with disaggregated Aβ fibril by EGCG, EGCG@Se, or Tet-1-EGCG@Se for 48 h, fixed with 4.0% paraformaldehyde, and then permeabilized with 0.1% Triton X-100 in PBS. The cells were incubated with a TUNEL reaction mixture for 1 h. For nuclear staining, cells were incubated with 1 μg mL^{-1} DAPI for 15 min at 37 °C. Stained cells were then washed with PBS and examined on a fluorescence microscope.

2.15. Determination of the Cellular Uptake of NPs. ICP-AES analysis was used to study the cellular uptake of the Tet-1-coated and -uncoated EGCG-stabilized NPs. The experiment was conducted in NIH/3T3 and PC12 cells. Briefly, cells were grown to attain a confluence of 10^7 cells. NPs (Tet-1-coated and -uncoated) were added to the cells and incubated for 12 h. After the incubation period, the cells were washed twice with PBS to remove all of the unbound NPs. The collected cells were digested with 3 mL of concentrated nitric acid and 1 mL of H_2O_2 in an infrared rapid digestion system (Gerhardt) at 180 °C for 1.5 h. The digested solution was reconstituted to 10 mL with Milli-Q water and used for ICP-AES analysis.

2.16. Intracellular Aβ Aggregate Detection. In order to assess whether the NPs could inhibit aggregation of Aβ inside PC12 cells, intracellular Aβ aggregate detection was performed. Briefly, cells were grown on coverslips, pretreated with an Aβ monomer for 6 h, allowing access of Aβ to the cytoplasm, sequentially incubated with EGCG, EGCG@Se, or Tet-1-EGCG@Se for 48 h, and then fixed in 4.0% paraformaldehyde for 10 min at room temperature. Cells were then incubated with a 0.05% solution of ThT and DAPI (1 μg mL^{-1}) and washed to remove any excessive stain. Coverslips were then mounted and analyzed by fluorescence microscopy (Axiophot, Zeiss)

3. RESULTS AND DISCUSSION

3.1. Preparation and Characterization of NPs. Scheme 1 illustrates the synthesis strategy for Tet-1-EGCG@Se. First, NPs were characterized by TEM and AFM. As indicated in Figure 1A−C, our NPs were characterized by monodispersion and homogeneous spherical structures, with an average diameter between 25 and 29 nm (Figure S1A in the Supporting Information, SI) as measured by a Nano-ZS instrument.

Variances in the reactant ratios can significantly affect both the diameter and morphology of SeNPs. When the ratio of EGCG to Na_2SeO_3 was less than that required for the reaction, EGCG acted predominantly as a reducing agent. This resulted

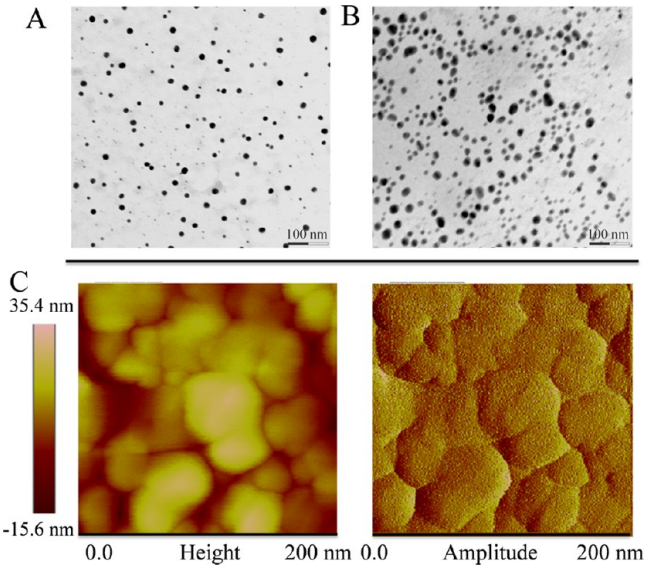

Figure 1. Morphological characterization of NPs. Negative TEM images of EGCG@Se (A) and Tet-1-EGCG@Se (B). Scar bar: 100 nm. (C) AFM image of Tet-1-EGCG@Se. Scar bar: 200 nm.

in an attenuated ability to act as a surface modifier, thus rendering it unable to form homogeneous and spherical SeNPs. However, when the reactant ratio was increased to 6:1, EGCG acted as both a reducing agent and a surface modifier, thereby able to control the formation of monodispersed and homogeneous spherical NPs. Finally, when the reactant ratio was increased to greater than 6:1, excessive EGCG was conjugated on the surface of the original Se crystal nucleus. This resulted in aggregation of the Se nuclei, ultimately leading to aggregation of the NPs. This change in morphology was accompanied by a color change for the solution, going gradually from transparency to pink and, finally, to brown (Figure S2 in the SI). This color transition was further validated from the UV−vis absorption spectra, as shown in Figure 2A. The absorbance bands at approximate 285 and 281 nm were observed in the spectra of EGCG@Se and Tet-1-EGCG@Se, respectively. Furthermore, the red shift from 275 to 285 nm (EGCG) or from 278 to 281 nm (Tet-1 peptide) indicated the inclusion of both EGCG and Tet-1 peptide in the fully synthesized NPs.[38]

To examine the effects of EGCG and Tet-1 peptide on the surface properties and stability of the SeNPs, we measured the ζ potential of EGCG@Se and Tet-1-EGCG@Se. As shown in Figure S1B in the SI, the ζ potential of EGCG@Se was −29.0 mV, which increased to 12.5 mV after Tet-1 peptide was coated on the surface. This characteristic serves to explain the robust stability of the two NPs. In further support of this stability, we also found that EGCG@Se and Tet-1-EGCG@Se remained stable for at least 9 days when stored in PBS buffer (Figure S3 in the SI). However, when the reaction time was increased to 10 days, the size of Tet-1-EGCG@Se dramatically increased to about 140 nm, and aggregation of critical nuclei occurred. As shown in Figure 2B, further elemental composition analysis was carried out using SEM-EDX. These data revealed a strong signal from the Se atoms (40.9%), together with C (30.8%), N (10.2%), and O (18.1%) atoms. No obvious peaks for other elements or impurities were observed. The presence of N atoms indicated that Tet-1 peptide successfully coated the surface of EGCG@Se.

SeNPs were further characterized by FT-IR to confirm the existence of chemical bonds. As shown in Figure 2C, the FT-IR spectra of EGCG@Se and Tet-1-EGCG@Se resemble those of EGCG and Tet-1 peptide, respectively, giving clear evidence that both EGCG and Tet-1 peptide form parts of the nanocomposite. In the spectrum of EGCG@Se, the peaks at 3360, 1620, and 1150 cm^{-1} were assigned to the stretching vibrations of −OH, O═C−O, and C−O, which corresponded to the analogous stretching vibrations of EGCG. The appearance of the above peaks as well as the addition of the peaks at 1700, 1640, and 1380 cm^{-1} in the spectrum of Tet-1-EGCG@Se further confirmed the presence of Tet-1 on the surface of the SeNPs.[39] Moreover, the characteristic peak of the −OH group in EGCG@Se and Tet-1-EGCG@Se nanocomposites at 3360 cm^{-1} was relatively lower than that of EGCG alone, indicating that EGCG was conjugated to the surface of SeNPs through this functional group.

To quantify Tet-1 peptide in Tet-1-EGCG@Se, we used a trace BCA kit assay. As shown in Table 1, the adsorption efficiency attained its maximum (78.8%) when the final concentration was increased to 10 μg mL^{-1}. Under these conditions, the calculated ratio of EGCG@Se to Tet-1 peptide was approximately 1:36 (based on the molarity).

Table 1. Adsorption Efficiency of Tet-1 Peptides with Different Initial Tet-1 Peptide Concentrations

	concn (μg mL^{-1})			
	2	4	10	16
adsorption efficiency (%)	66.1 ± 4.2	73.5 ± 4.0	78.8 ± 3.9	41.0 ± 3.1

3.2. Effect of NPs on Aβ Aggregation. It has been shown that AD arises primarily from protein conformational disorder (PCD). In PCD, a given protein misfolds and causes a change

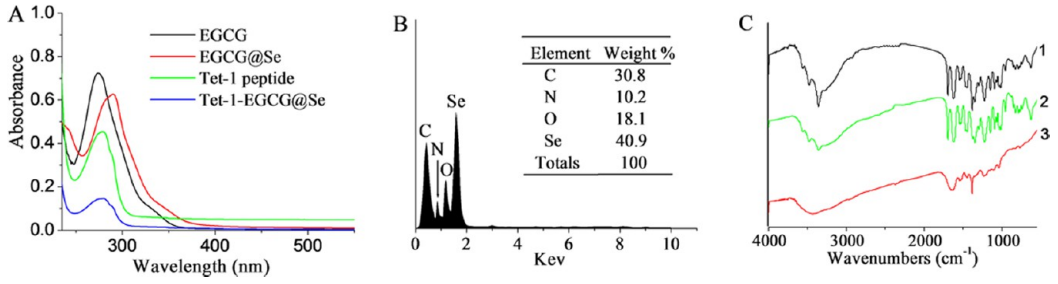

Figure 2. Chemical composition characterization of EGCG@Se and Tet-1-EGCG@Se: (A) UV spectra of EGCG@Se and Tet-1-EGCG@Se; (B) EDX analysis of Tet-1-EGCG@Se; (C) FT-IR spectra of EGCG (1), EGCG@Se (2), and Tet-1-EGCG@Se (3).

dx.doi.org/10.1021/am501341u | ACS Appl. Mater. Interfaces 2014, 6, 8475−8487

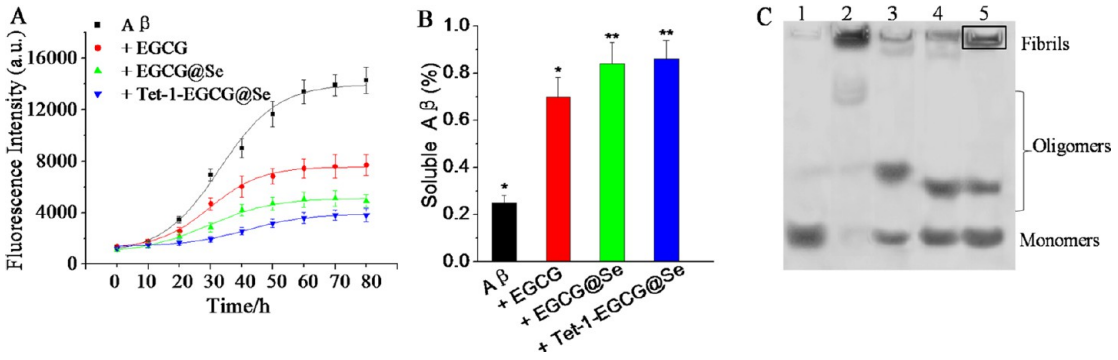

Figure 3. (A) Fibrillation kinetics of Aβ as monitored by the development of ThT binding in the presence of EGCG, EGCG@Se, and Tet-1-EGCG@Se. (B) Percentage of soluble Aβ in the absence and presence of EGCG, EGCG@Se, or Tet-1-EGCG@Se: (*) $p < 0.05$ and (**) $p < 0.01$, respectively. (C) Determination of the Aβ monomer (1) and the formation of Aβ fibrils in the absence (2) or presence of EGCG (3), EGCG@Se (4), and Tet-1-EGCG@Se (5) by native PAGE. Samples were prepared as described in the Experimental Section.

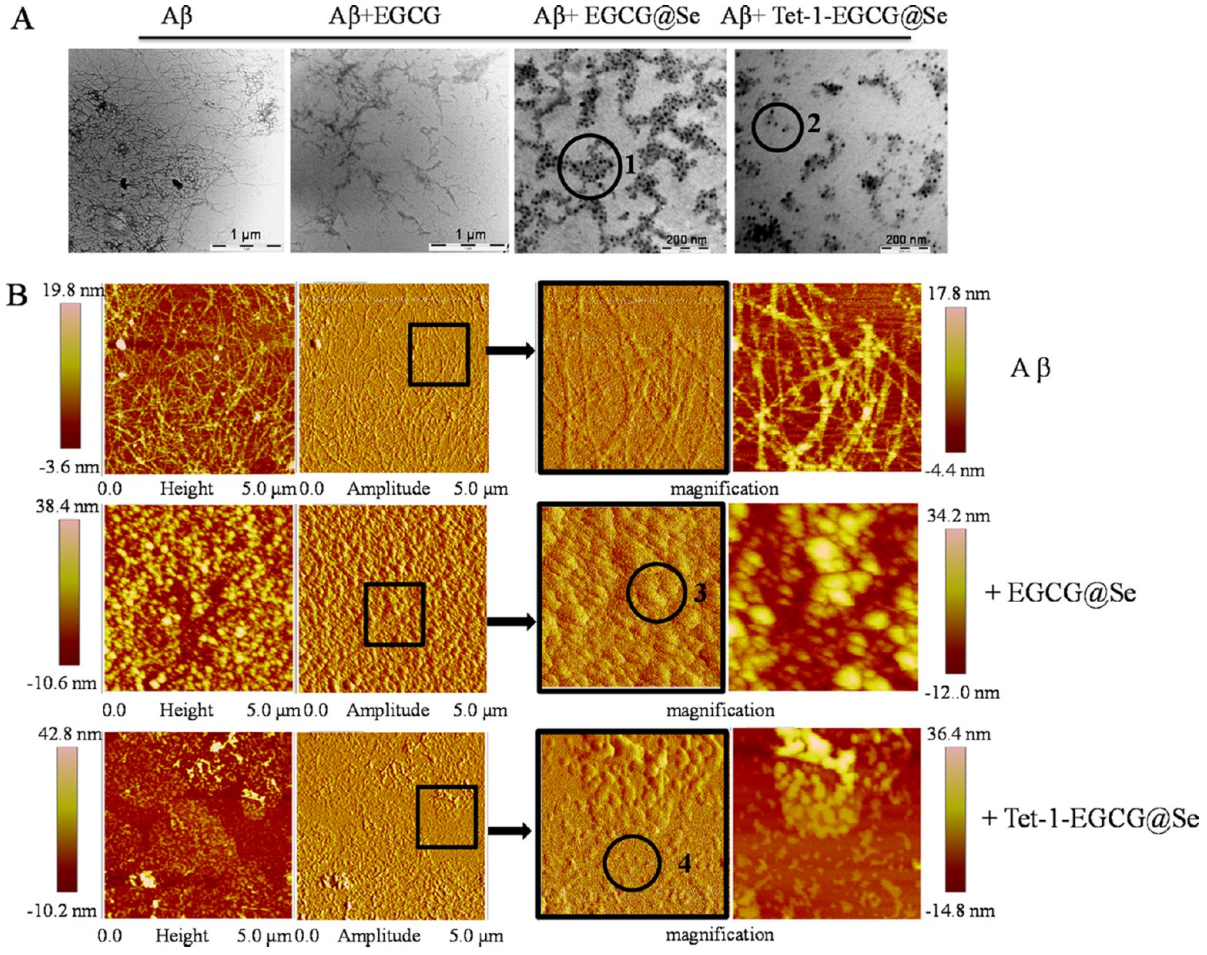

Figure 4. Morphological analysis of Aβ aggregates. (A) TEM images of Aβ aggregates forming in the absence or presence of EGCG, EGCG@Se, and Tet-1-EGCG@Se. (B) AFM analysis of Aβ aggregation in the absence or presence of EGCG@Se and Tet-1-EGCG@Se. Left images are 5 × 5 μm^2. The right images are the corresponding magnification areas marked with black frames. The circles indicate the morphologies of Aβ aggregates.

in its secondary or tertiary structure without altering its primary structure.[40] For instance, in AD a conformational change in Aβ from a random-coil to a β-sheet structure occurs prior to Aβ fibril formation. Quantitatively, ThT fluorescence has been widely used to detect these β-sheet structure conformers and their Aβ aggregates.[41,42] By binding to the aggregated β-sheet fibrils common to amyloid structures, ThT gives rise to a significant increase in its fluorescence.[43] This property of ThT gives it a particular usefulness to examine the inhibitory effect of our NPs on Aβ fibrillation.

We first used ThT fluorescence to detect aggregated β-sheet fibrils in the presence of EGCG, EGCG@Se, and Tet-1-EGCG@Se (10 μg mL^{-1}). As shown in Figure 3A, Aβ produced a typical sigmoidal curve, showing the kinetics of amyloid fibrils formed in PBS at 37 °C. As hypothesized, this observed behavior was opposite to the behavior that we observed when Aβ was in the presence of either EGCG@Se or

dx.doi.org/10.1021/am501341u | ACS Appl. Mater. Interfaces 2014, 6, 8475−8487

Tet-1-EGCG@Se. Under these conditions, the kinetics of Aβ fibril growth was delayed and initiated after only 30 h (EGCG@Se) and 40 h (Tet-1-EGCG@Se). Additionally, the ThT fluorescence intensity achieved a maximum level of nearly 4000 au with Aβ incubated with Tet-1-EGCG@Se and 5000 au in those incubated with EGCG@Se. Conversely, this behavior was not seen in Aβ treated with EGCG alone. Under these conditions, half transformed into amyloid fibrils compared to the control. Collectively, these results indicate that both EGCG@Se and Tet-1-EGCG@Se improved the inhibitory efficacy of EGCG on Aβ aggregation.

We further studied the inhibitory action of NPs on Aβ aggregation by measuring the amount of soluble Aβ in the supernatant of the reaction mixtures using native PAGE. In the absence of inhibitors, Aβ was almost completely insoluble (Figure 3B). However, soluble Aβ increased to 78% and 82% in the supernatant of Aβ reaction mixtures containing EGCG@Se and Tet-1-EGCG@Se, respectively. In the presence of a similar concentration of EGCG alone, soluble Aβ reached only 59% of its initial amount.

Aβ solutions were prepared for ThT fluorescence assay and were subjected to native PAGE (Figure 3C). After being incubated for 48 h in PBS buffer, Aβ alone presented a heavy band and a faint band, indicating a fibril and a monomer component, respectively (Figure 3C, line 2). In the case of coincubation with Tet-1-EGCG@Se (Figure 3C, line 5), the fibrous band disappeared and the monomer bands were much more intense than those for either the EGCG (Figure 3C, line 3) or EGCG@Se group (Figure 3C, line 4). Of note, the presence of Tet-1-EGCG@Se accounts for the intense band indicated in line 5 (Figure 3C). Simultaneously, several oligomers appeared in the presence of different inhibitors. Interestingly, the smallest oligomers formed only when the peptide was coincubated with Tet-1-EGCG@Se. Given these data, it is plausible that Tet-1-EGCG@Se can inhibit Aβ aggregation by inducing the formation of small oligomers in their place.[11] In general, the above results indicate that the introduction of NPs into Aβ substantially inhibits Aβ aggregation. It is possible that one reason why Tet-1-EGCG@Se performs better than EGCG or EGCG@Se may be attributable to their positive charge and their hydrophobic interactions between Tet-1 and Aβ. However, further studies will be needed to investigate this hypothesis.

3.3. Ultrastructural and Cytotoxic Analyses of NP-Induced Aβ Oligomerization. We used TEM analysis to determine the NPs' inhibitory effect on the ultrastructural properties of assembled Aβ oligomers. As shown in Figure 4A, Aβ samples incubated for 48 h without inhibitors formed large, branched fibrils. Samples of Aβ containing EGCG (10 μg mL^{-1}) showed aggregates similar to those observed in control samples but formed to a smaller degree. Aβ samples containing either EGCG@Se or Tet-1-EGCG@Se contained mostly spherical particles and amorphous oligomers with negligible amounts of short fibrils. It should be noted that the observed spherical particles are nearly equal in diameter to the NPs, which suggests the possibility that NPs decrease Aβ aggregation by constraining the protein in its native-like state (e.g., monomers and amorphous oligomers).[19,44] Importantly, amorphous oligomers induced by Tet-1-EGCG@Se (Figure 4A, circle 1) were significantly smaller than those induced by EGCG@Se (circle 2).

To corroborate the findings of the ThT and TEM experiments, we used AFM to monitor fibril formation at 37 °C in the presence or absence of EGCG@Se or Tet-1-EGCG@Se (10 μg mL^{-1}; Figure 4B). As hypothesized, Aβ alone showed distinct fibrillar networks with defined elongated structure and the introduction of NPs obviously inhibited the fibrillation of Aβ, resulting in the formation of amorphous oligomers (Figure 4B, circles 3 and 4). These results correlate with and corroborate the results of our ThT fluorescence and TEM assays.

We used cytotoxicity assay to further investigate the properties of NP-induced Aβ oligomers. As shown in Figure 5, EGCG@Se (10 μg mL^{-1}) and EGCG (10 μg mL^{-1}) were

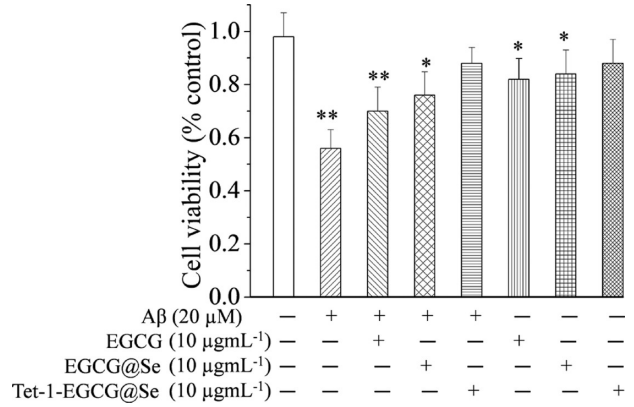

Figure 5. Reduction in the metabolic activity of PC12 cells by Aβ monomers in the absence and presence of EGCG, EGCG@Se, and Tet-1-EGCG@Se, (*) $p < 0.05$ and (**) $p < 0.01$, respectively, indicating significant and very significant differences between the treated and control cells.

both able to partially reduce the cytotoxicity induced by Aβ in PC12 cells. However, Tet-1-EGCG@Se (10 μg mL^{-1}) substantially increased the cell viability from 0.56 to 0.88 (% of control), indicating that the formation of amorphous amyloid oligomers correlates with reduced cellular toxicity.

On the basis of our ThT, TEM, AFM, and cytotoxicity analyses, there is significant evidence that Tet-1-EGCG@Se can effectively mitigate Aβ fibrillation. This effect is hypothesized to occur by constraining the protein in its native-like state, which consists primarily of monomers and nontoxic amorphous oligomers. Comparatively, both EGCG and EGCG@Se are less effective at inhibiting Aβ fibrillation and subsequently rescuing Aβ-induced cytotoxicity.

3.4. Disaggregation of Preformed Aβ Fibrils by NPs. After investigating the impact of NPs on the aggregation of Aβ, we decided to investigate the NPs' potential for fibril disaggregation. To test the hypothesis that these NPs bind to fibrils uniformly and then allow for their disaggregation, we first checked the binding ability of the NPs by incubating Aβ fibrils with 10 μg mL^{-1} EGCG@Se or Tet-1-EGCG@Se. At defined time intervals of 1 h, small aliquots of solution were sampled and the binding was measured. We observed that both EGCG@Se and Tet-1-EGCG@Se had a high affinity for the fibrils and bound rapidly after their addition (data are not shown). No differences were observed within 6 h (Figure 6A). To verify the specificity of the interaction between the NPs and Aβ fibrils, we performed specificity assay using CA@Se. After 12 h of incubation, CA@Se neither bound to nor changed the fibrils (Figure S4 in the SI). These data provided preliminary evidence that both EGCG@Se and Tet-1-EGCG@Se have high and specific affinities for Aβ fibrils.[45]

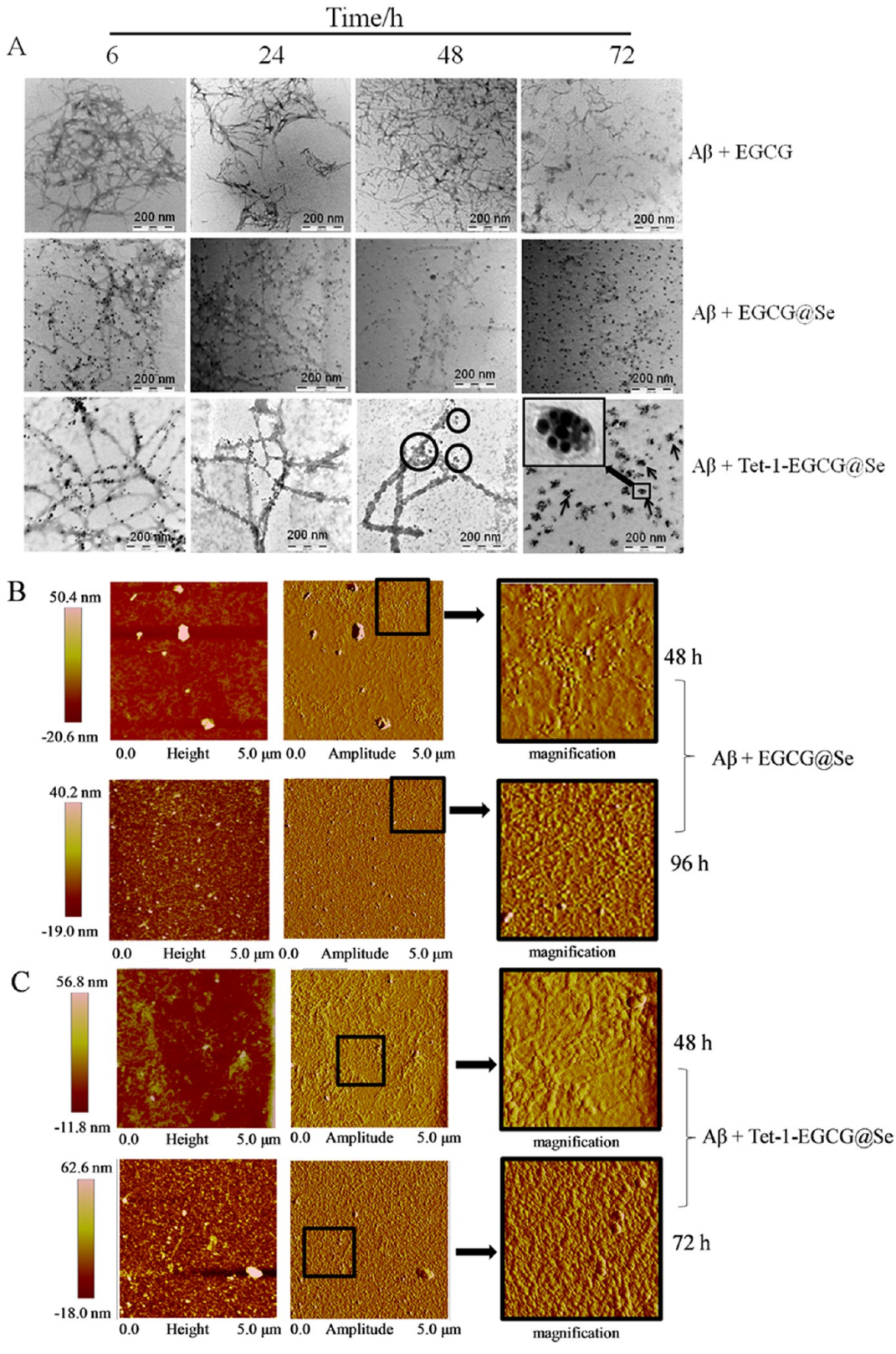

Figure 6. Disaggregation of Aβ fibrils by EGCG, EGCG@Se, and Tet-1-EGCG@Se. Aβ fibrils were prepared as described in the Experimental Section. Aβ fibrils were incubated with EGCG, EGCG@Se, and Tet-1-EGCG@Se (10 μg mL^{-1}) in PBS at 37 °C. After 6–96 h of incubation, samples were examined by TEM (A) and AFM (B and C) at different incubation times. (B) Disaggregation by EGCG@Se observed by AFM after 48 and 96 h. (C) Disaggregation of Aβ fibrils by Tet-1-EGCG@Se observed under AFM after 48 and 72 h. Black arrows indicated the formation of spherical aggregates containing 5–8 individual NPs. The left images are 5 × 5 μm^2. The right images are the corresponding magnification areas marked with black frames.

dx.doi.org/10.1021/am501341u | ACS Appl. Mater. Interfaces 2014, 6, 8475–8487

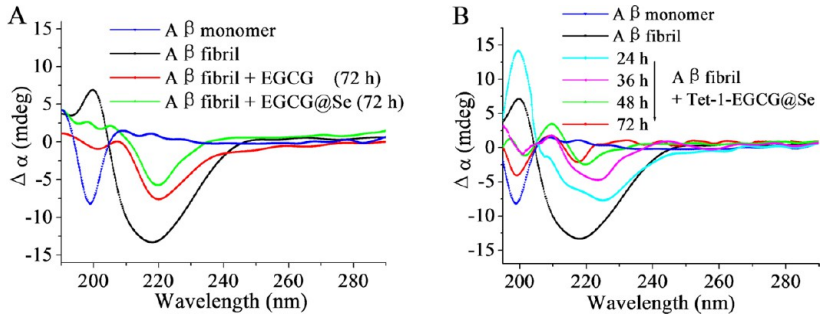

Figure 7. Secondary structure analysis of Aβ fibrils by CD spectra: (A) changes in the secondary structure of Aβ following incubation at 37 °C for 72 h in the absence and presence of EGCG and EGCG@Se; (B) restoration in the secondary structure of Aβ following incubation at 37 °C for 24−72 h in the presence and absence of Tet-1-EGCG@Se.

Having established a NP binding affinity for Aβ fibrils, we then examined EGCG@Se- or Tet-1-EGCG@Se-mediated fibril disaggregation. To do so, Aβ fibrils were incubated with EGCG, EGCG@Se, or Tet-1-EGCG@Se for 72 h at 37 °C in PBS. After 24, 48, and 72 h, small aliquots of the reaction mixture were withdrawn and TEM was used to detect the extent of fibril disaggregation. As illustrated in Figure 6A, disaggregation of fibrils mediated by either EGCG or EGCG@Se at 24 h was negligible. However, disaggregation of fibrils by Tet-1-EGCG@Se was clear after only 24 h of incubation. After 48 h of incubation, we observed that treatment with Tet-1-EGCG@Se resulted in the expulsion of degradative products from the fibrils, indicated by the black circles in Figure 6A. At this same time point, EGCG@Se was found to have disaggregated many long fibrils, whereas EGCG still had no effect. At 72 h of incubation, only spherical aggregates (indicated by the arrows in Figure 6A) were observed in fibrils treated with Tet-1-EGCG@Se. Because there were no visible fibrils at this time point, we concluded that all fibrils were completely disaggregated. At this same time point, EGCG@Se was found to have reduced most long fibrils to shortened fibrils, which were then remodeled into amorphous structures. Of note is that treatment with Tet-1-EGCG@Se created spherical aggregates that contained nonisolatable particles of 5−8 nm diameter. These aggregates are either new NPs that have been modified by disaggregated fibrils or broken fibrils themselves that have bound Tet-1-EGCG@Se.

It is reported that EGCG can interfere with the aromatic hydrophobic core of Aβ. The C-terminal part of the Aβ peptide (residues 22−39) adopts a β-sheet conformation, while the N-terminus (residues 1−20) is unstructured. EGCG interacts in solution with the unfolded Aβ peptide via aromatic interactions, thus causing a change in the structure of Aβ fibrils.[19,44] Also, according to our results, the interactions between NPs and Aβ fibrils might be enhanced by the presence of a Se atom and Tet-1 peptide. We can explain by assuming the fact that EGCG@Se increases the local concentration of EGCG and the presence of Tet-1 peptide allows a stronger aromatic interaction between Tet-1-EGCG@Se and Aβ fibrils. As for the spheroidal aggregates, we presume they are either new NPs modified by disaggregated fibrils or broken fibrils tangled with Tet-1-EGCG@Se.

We sought to further verify NP-induced fibril disaggregation via AFM. As shown in Figure 6B, at 96 h, EGCG@Se had significantly disaggregated all fibrils. This rate of disaggregation was found to be slower than that induced by Tet-1-EGCG@Se. As illustrated in Figure 6C, by 48 h, most of the fibrils had been disaggregated into fragments. Additionally, TEM revealed that these individual fragments had been transformed into smaller, spheroidal spherical aggregates after 72 h of incubation.

Given these results, we then investigated the secondary structure of the disaggregated fibrils through the use of CD spectroscopy. As indicated earlier, Aβ that has been freshly dissolved in a buffer solution exhibits a typical CD spectrum of the random-coil conformation with a maximum negative mean residue ellipticity below 200 nm (Figure 7A, blue line). However, the Aβ fibril shows the maximum negative mean residue ellipticity at 218 nm, thus indicating the presence of a main β-sheet structure (Figure 7A, cyan line). As shown in Figure 7A, after 72 h of coincubation of fibrils with EGCG or EGCG@Se, the conformation conversion of Aβ peptides was still not clear. This is evidenced by an apparent negative band at 217 nm, which is similar to that seen with the Aβ fibril alone. Intriguingly, after the addition of Tet-1-EGCG@Se to the Aβ fibrils, the spectrum shifts to one typical of a random-coil conformation. This shift appears gradually and overlaps the spectrum of Aβ monomers. At 24 and 36 h, the spectrum appears as a broad, negative band around 218 nm, a positive band at 195 nm, and a negative band at 195 nm (Figure 7B). These three distinct bands can be attributed to the mixture of random-coil, β-sheet, and α-helix structures, respectively.[46] After 72 h of incubation, the fibril had mostly reverted back to a random-coil conformation. Taken together, these results suggest that Tet-1-EGCG@Se succeeds in converting the β-sheet-rich fibrils into amorphous aggregates that exhibit a random-coil conformation.

Finally, the disaggregated Aβ fibrils were added to PC12 cells to determine their effects on the cytotoxicity. Tet-1-EGCG@Se was found to significantly reduce the cytotoxicity of the fibrils (Figure S5 in the SI). Moreover, fibrils that had been disaggregated by EGCG@Se were also less toxic to PC12 cells. However, this reduction in the cytotoxicity was not observed when EGCG-only-treated aggregates were added to PC12 cells. Thus, our data indicate that remodeling of the amyloid fibrils with EGCG@Se and Tet-1-EGCG@Se correlates with reduced cellular toxicity. Conversely, EGCG administered at the same concentration did not alter the cytotoxicity of preformed amyloid fibrils.

Generally, Tet-1-EGCG@Se remodels fibrils into spherical aggregates that have been shown to be nontoxic. Importantly, self-association of the hydrophobic core region with its amino acids is critical for spontaneous amyloid polymerization.[45] It is thus tempting to speculate that the broad interaction with this region damages the fibrillar structure. For instance, although bearing a surface area similar to that of Tet-1-EGCG@Se, EGCG@Se is relatively less effective in disaggregating the fibril.

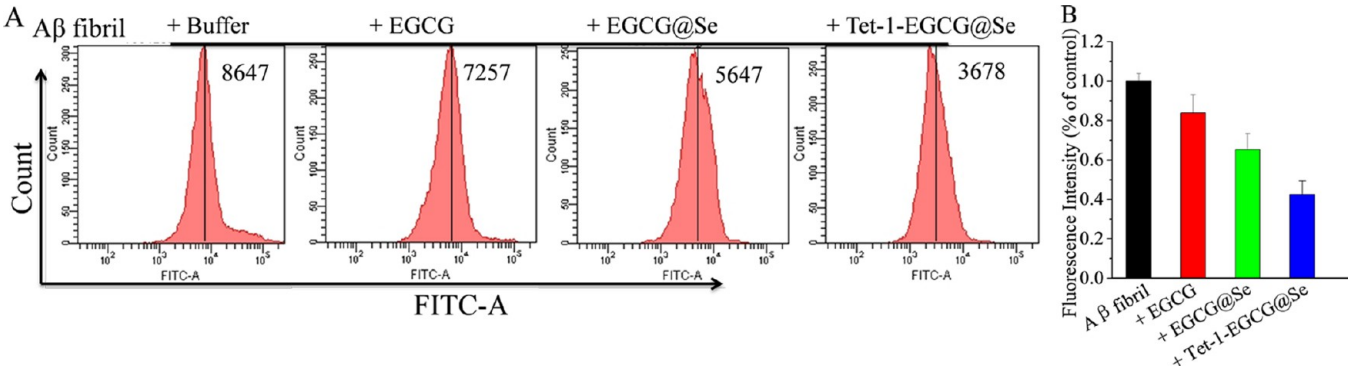

Figure 8. Detection of ROS production induced by Aβ fibrils in PC12 cells. (A) Aβ fibrils were incubated in PBS buffer for 72 h (pH = 7.4, 37 °C) in the absence or presence of EGCG, EGCG@Se, and Tet-1-EGCG@Se, respectively. Then the samples were added to PC12 cells for an additional 24 h of incubation. The ROS level was quantified by the fluorescence of DCF (488 nm excitation and 530 nm emission). (B) Quantitative analysis of the ROS level presented by the DCF fluorescence intensity. The data shown here are representative of three independent experiments with similar results.

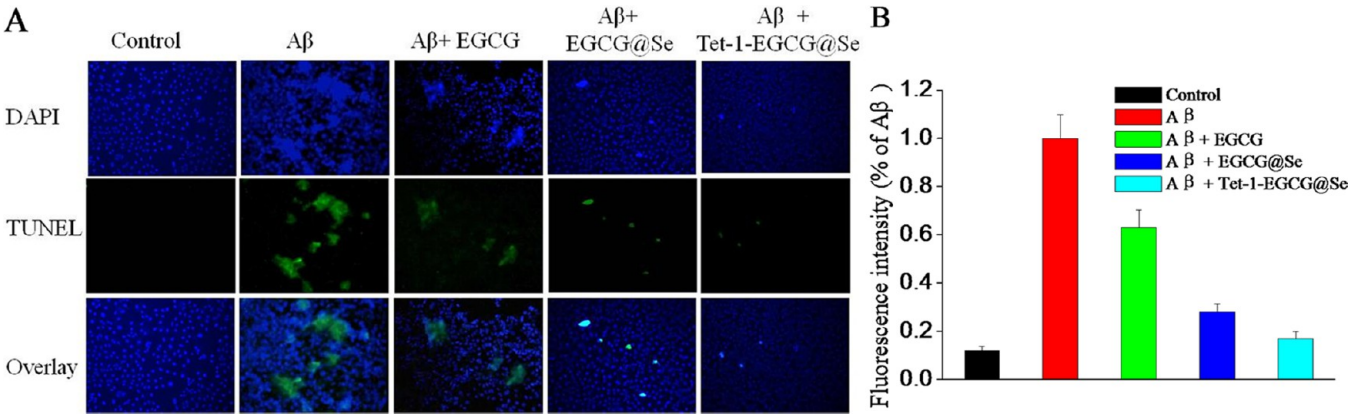

Figure 9. DNA fragmentation and nuclear condensation induced by disrupted Aβ fibrils in the absence and presence of EGCG, EGCG@Se, and Tet-1-EGCG@Se in PC12 cells. (A). Cells were treated with disrupted Aβ fibrils for an additional 24 h, and the result was detected by TUNEL−DAPI costaining assay. (B) Quantitative analysis of DNA fragmentation presented by the TUNEL fluorescence intensity. The values expressed are the mean ± standard deviation in triplicate.

It is known that Tet-1 ligands possess more H-bond sites, which therefore may be able to interact more with the Aβ fibrils. Furthermore, it has been revealed that the relatively high density of negative charges on the surface of the NPs may repel the Aβ with net negative charges of at least −3, thus retarding the interactions between EGCG@Se and the Aβ fibrils. Contrastingly, EGCG-treated fibrils are a heterogeneous mixture of amorphous aggregates and broken amyloid fibrils. While this is likely due to the reduced H-bond sites in EGCG, which would result in weaker hydrophobic interactions with Aβ fibrils, further studies are needed to validate this hypothesis.

3.5. NPs Reduced Aβ-Fibril-Induced ROS Generation in PC12 Cells. Because the toxicity of Aβ is mainly mediated by Aβ-fibril-induced ROS,[47] we hypothesized that these NPs would be able to reduce cell death through its antioxidant antiaggregation properties. PC12 cells were treated with the Aβ fibril and then allowed to disaggregate upon incubation with EGCG, EGCG@Se, or Tet-1-EGCG@Se. We then examined intracellular ROS generation in PC12 cells by measuring the DCF fluorescence intensity. This assay allows for accurate readings of the ROS levels by allowing for the cellular uptake of a nonfluorescent probe (DCFH-DA), which is subsequently hydrolyzed by intracellular esterase to form dichlorofluorescien (DCFH).

As shown in Figure 8, Tet-1-EGCG@Se treatment (10 μg mL^{-1}) and the resulting disaggregated Aβ fibril decreased the DCF fluorescence intensity from 8647 to 3678 au. This shift in the intensity indicates a down-regulation of intracellular ROS levels induced by Aβ fibrils. Incubation with EGCG@Se (10 μg mL^{-1}) showed a markedly reduced ability at decreasing the Aβ-induced ROS levels, with the fluorescence intensity shifting to only 5647 au. However, in the presence of EGCG, the fluorescence intensity was still relatively high (7257 au), suggesting a slight change of the ROS level compared to that induced by Aβ fibrils. Collectively, these results suggest that induced ROS levels can be decreased by both EGCG@Se and Tet-1-EGCG@Se to a certain extent. Furthermore, these data indicate that EGCG@Se and Tet-1-EGCG@Se are capable of transforming Aβ fibrils into structures that induce less ROS in the PC12 cells.

3.6. TUNEL and DAPI Costaining Assay. To further study the disaggregated Aβ fibrils, we applied disaggregated Aβ fibrils to PC12 cells to test whether they would directly cause cell apoptosis. We then performed an in vitro TUNEL enzymatic labeling and DAPI costaining assay to determine the extent of DNA fragmentation and nuclear condensation. As previously described, TUNEL can detect the early stages of DNA fragmentation in apoptotic cells prior to more overt changes in the cellular morphology.[48] As shown in Figure 9, Aβ

fibrils caused a significant increase in DNA fragmentation and nuclear condensation in PC12 cells (green and blue colors corresponding to TUNEL and DAPI staining, respectively). However, in the presence of Aβ fibrils disaggregated by either EGCG@Se or Tet-1-EGCG@Se (10 μg mL^{-1}), we observed a significant decrease in DNA fragmentation. EGCG at the same concentration was found to only slightly decrease the amount of DNA fragmentation. Usually amyloid fibrils form and deposit in the vicinity of the target cells and accumulate on the cell membrane, triggering a cascade of cellular events that lead to apoptosis, which was also clearly shown in cells treated with Aβ fibril with or without EGCG. These results clearly demonstrate that both EGCG@Se and Tet-1-EGCG@Se can transform Aβ fibrils to a structure that lessens the induction of DNA fragmentation in PC12 cells. Furthermore, these results are consistent with our data from ROS assay, indicating a decrease in the overall Aβ-fibril-induced cytotoxicity and possible apoptotic activity in cells treated with either EGCG@Se or Tet-1-EGCG@Se. However, it requires further studies to validate the necrosis induced by the Aβ fibril because necrosis is always accompanied by Aβ-fibril-induced cytotoxicity.

3.7. In Vitro Uptake Study. The activity of a drug is just as important to its functioning as its proper delivery to its site of action. To this end, we used ICP to better understand the in vitro uptake of both targeted and nontargeted NPs intracellularly. To investigate the delivery efficiency of EGCG@Se and Tet-1-EGCG@Se in neuronal cells, we assessed the cellular uptake of NPs in both NIH/3T3 and PC12 cells using ICP-AES analysis.

As shown in Figure 10, PC12 cells treated with 5 and 10 μg mL^{-1} Tet-1-EGCG@Se had significantly increased Se concentrations, from 0.09 (control) to 2.80 and 5.60 μg/10^7 cells. This increase was significantly higher than that seen for NPs without Tet-1 peptide (1.40 μg/10^7 cells even at 10 μg mL^{-1} concentration). However, similar results were not seen in NIH/3T3 cells. Even at high concentrations, Tet-1-EGCG@Se permeated NIH/3T3 cells to a low degree. Conversely, EGCG@Se was observed to accumulate in NIH/3T3 cells at a relatively high concentration (1.2 μg/10^7 cells). Our results suggest that Tet-1 targeting increased the neuronal uptake of Tet-1-EGCG@Se compared to the nontargeted NPs in PC12 cells. This effect was not seen for NIH/3T3 cells. It is reported that Tet-1 peptide can recognize trisialoganglioside-GT1b (i.e., a natural receptor on the surface of a neuron). Because a PC12 cell membrane contains sufficient GT1b, Tet-1-EGCG@Se can easily be recognized and endocytosed by PC12 cells rather than by NIH/3T3 cells.[32]

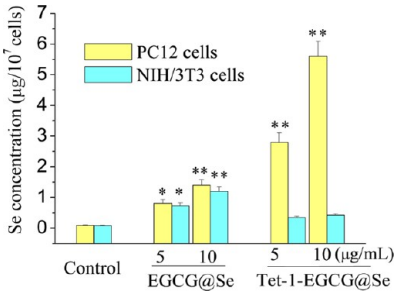

Figure 10. Quantitative analysis of Se concentrations in PC12 and NIH/3T3 cells exposed to EGCG@Se and Tet-1-EGCG@Se for 12 h by the ICP-AES method, (*) $p < 0.05$ and (**) $p < 0.01$, respectively, indicating significant and very significant differences between the treated and control cells. The values expressed are the mean ± standard deviation in triplicate.

Our results indicate that Tet-1 targeting can be used for drug delivery that is specific to neurons, thereby allowing for increased drug efficiency and targeting selectivity.

3.8. Detection of Aβ Fibrillation inside PC12 Cells by a Fluorescence Microscope. To further investigate Aβ fibrillation inside PC12 cells, we carried out fluorescence assay in the presence of either EGCG@Se or Tet-1-EGCG@Se. First, we pretreated PC12 cells with an Aβ monomer for 6 h to allow the uptake of Aβ into the cytoplasm.[49] We then sequentially added EGCG, EGCG@Se, or Tet-1-EGCG@Se (10 μg mL^{-1}) to the cells for an additional 48 h of incubation. Cells were then incubated with a 0.05% solution of ThT and DAPI (1 μg mL^{-1}) and washed to remove any excess stain. As previously described, the Aβ fibril is easily labeled by ThT, so we were able to estimate the degree of intracellular Aβ fibrillation by assessing the intensity of ThT fluorescence. As shown in Figure 11, significant Aβ fibrillation was observed in the presence of Aβ alone. When the cells were coincubated with either EGCG or EGCG@Se, the ThT fluorescence intensity decreased but was still visible. However, in the presence of Tet-1-EGCG@Se, there was a near-complete reduction of ThT fluorescence. Taken together, these results indicate that both EGCG and EGCG@Se are less effective against Aβ fibrillation in PC12 cells. However, Tet-1-EGCG@Se can effectively inhibit Aβ fibrillation inside the PC12 cells. Furthermore, we hypothesize that the enhanced cellular uptake of Tet-1-EGCG@Se contributes to its significantly increased inhibition of Aβ fibrillation in PC12 cells.

4. CONCLUSIONS

Our results suggest that Tet-1-EGCG@Se is a potential therapeutic candidate for the labeling and disaggregating of Aβ fibrils. Both EGCG@Se and Tet-1-EGCG@Se can inhibit Aβ aggregation by causing aggregate disruption and the formation of small oligomers. Tet-1-EGCG@Se can effectively mitigate Aβ fibrillation by constraining the protein to its native-like state, which is constituted by monomeric and nontoxic amorphous oligomeric species. While EGCG and EGCG@Se are less effective at inhibiting Aβ fibrillation and rescuing the cytotoxicity induced by Aβ, we have found that Tet-1-EGCG@Se can remodel Aβ fibrils into spherical aggregates that are nontoxic and have a non-β-sheet structure. Interestingly, EGCG@Se and Tet-1-EGCG@Se have a high specific affinity for Aβ fibrils. However, the mechanism by which this fibril disaggregation occurs has yet to be fully elucidated.

Our in vitro study also demonstrated that Tet-1-EGCG@Se is able to protect PC12 cells against Aβ-induced damage by suppressing the generation of ROS and DNA fragmentation. In addition, EGCG@Se can also disaggregate Aβ fibrils into low-toxicity aggregates, which was confirmed by both our ROS assay and TUNEL and DAPI costaining assay. We also found that tagging the EGCG-modified SeNP with Tet-1 neuropeptide greatly increases its in vitro neuronal targeting efficiency. Increasing its targeting ability would not only enhance its ability to localize to the site of delivery but also allow for greater overall drug efficacy. While these results are robust and promising, additional in vitro and in vivo studies will be needed to further validate these findings and better understand the anti-AD effects of these NPs in other model systems.

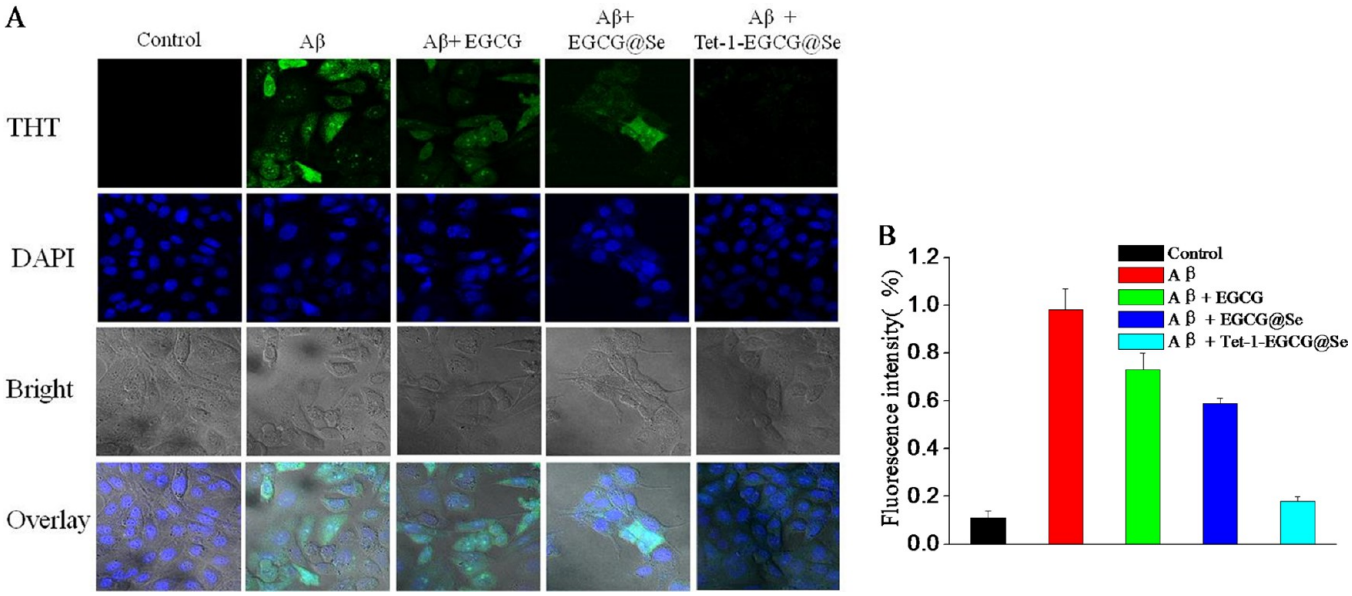

Figure 11. (A) Tet-1-EGCG@Se preventing Aβ aggregation in PC12 cells. The presence of intracellular Aβ fibrils was evaluated by ThT staining in PC12 cells in the absence and presence of EGCG, EGCG@Se, and Tet-1-EGCG@Se. The cells were pretreated with an Aβ monomer for 6 h to allow access of Aβ to the cytoplasm, sequentially incubated with EGCG, EGCG@Se, or Tet-1-EGCG@Se for an additional 48 h, and visualized under a fluorescence microscope. (B) Quantitative analysis of Aβ aggregation presented by the ThT fluorescence intensity. The values expressed are the mean ± standard deviation in triplicate.

■ ASSOCIATED CONTENT

Supporting Information

Size distribution (A) and ζ potential (B) of EGCG@Se and Tet-1-EGCG@Se, change in the color of NPs after EGCG functionalization, citric acid functionalization, and Tet-1 peptide coating, stability of EGCG@Se and Tet-1-EGCG@Se in PBS buffer (pH = 7.4) presented by size distribution, binding propensities of CA@Se to Aβ fibrils observed by TEM, and the cytotoxicity of the Aβ fibrils disaggregated by EGCG, EGCG@Se, and Tet-1-EGCG@Se in PC12 cells. This material is available free of charge via the Internet at http://pubs.acs.org.

■ AUTHOR INFORMATION

Corresponding Author

*E-mail: tliuliu@jnu.edu.cn. Tel/Fax: +86-20-85220223.

Author Contributions

†These authors contributed equally to the work.

Notes

The authors declare no competing financial interest.

■ ACKNOWLEDGMENTS

This work was supported by the National Natural Science Foundation of China (Grants 21171070 and 21371075), the Planned Item of Science and Technology of Guangdong Province (Grant c1211220800571), and the Natural Science Foundation of Guangdong Province and the Fundamental Research Funds for the Central Universities.

■ REFERENCES

(1) Kosik, K. S. Alzheimer's Disease: a Cell Biological Perspective. *Science* **1992**, *256*, 780−783.

(2) Yamin, G.; Ono, K.; Inayathullah, M.; Teplow, D. B. Amyloid−Protein Assembly as a Therapeutic Target of Alzheimers Disease. *Curr. Pharm. Des.* **2008**, *14*, 3231−3246.

(3) Rafii, M. S.; Aisen, P. S. Recent Developments in Alzheimer's DiseaseTherapeutics. *BMC Med.* **2009**, *7*, 7.

(4) Abbott, A. Dementia: a Problem for Our Age. *Nature* **2011**, *475*, S2−S4.

(5) Iqbal, K.; Grundke-Iqbal, I. Developing Pharmacological Therapies for Alzheimer Disease. *Cell. Mol. Life Sci.* **2007**, *64*, 2234−2244.

(6) Youdim, M. B.; Buccafusco, J. J. Multi-functional Drugs for Various CNS Targets in the Treatment of Neurodegenerative Disorders. *Trends Pharmacol. Sci.* **2005**, *26*, 27−35.

(7) Park, S.-Y.; Kim, H.-S.; Cho, E.-K.; Kwon, B.-Y.; Phark, S.; Hwang, K.-W.; Sul, D. Curcumin Protected PC12 Cells Against Beta-Amyloid-induced Toxicity Through the Inhibition of Oxidative Damage and Tau Hyperphosphorylation. *Food Chem. Toxicol.* **2008**, *46*, 2881−2887.

(8) Lim, G. P.; Chu, T.; Yang, F.; Beech, W.; Frautschy, S. A.; Cole, G. M. The Curry Spice Curcumin Reduces Oxidative Damage and Amyloid Pathology in an Alzheimer Transgenic Mouse. *J. Neurosci.* **2001**, *21*, 8370−8377.

(9) Chen, T.; Wang, X.; He, Y.; Zhang, C.; Wu, Z.; Liao, K.; Wang, J.; Guo, Z. Effects of Cyclen and Cyclam on Zinc (II)-and Copper (II)-induced Amyloid β-peptide Aggregation and Neurotoxicity. *Inorg. Chem.* **2009**, *48*, 5801−5809.

(10) Wang, X.; Wang, X.; Zhang, C.; Jiao, Y.; Guo, Z. Inhibitory Action of Macrocyclic Platiniferous Chelators on Metal-induced Aβ Aggregation. *Chem. Sci.* **2012**, *3*, 1304−1312.

(11) Geng, J.; Li, M.; Ren, J.; Wang, E.; Qu, X. Polyoxometalates as Inhibitors of the Aggregation of Amyloid β Peptides Associated with Alzheimer's Disease. *Angew. Chem.* **2011**, *123*, 4270−4274.

(12) Doss, M. X.; Potta, S. P.; Hescheler, J.; Sachinidis, A. Trapping of Growth Gactors by Catechins: a Possible Therapeutical Target for Prevention of Proliferative Diseases. *J. Nutr. Biochem.* **2005**, *16*, 259−266.

(13) Weinreb, O.; Amit, T.; Mandel, S.; Youdim, M. B. Neuroprotective Molecular Mechanisms of (−)-Epigallocatechin-3-gallate: a Reflective Outcome of its Antioxidant, Iron Chelating and Neuritogenic Properties. *Genes Nutr.* **2009**, *4*, 283−296.

(14) Biasibetti, R.; Tramontina, A. C.; Costa, A. P.; Dutra, M. F.; Quincozes-Santos, A.; Nardin, P.; Bernardi, C. L.; Wartchow, K. M.; Lunardi, P. S.; Gonçalves, C.-A. Green Tea (−)-Epigallocatechin-3-gallate Reverses Oxidative Stress and Reduces Acetylcholinesterase

Activity in a Streptozotocin-induced Model of Dementia. *Behav. Brain Res.* **2013**, *236*, 186−193.
(15) Rezai-Zadeh, K.; Arendash, G. W.; Hou, H.; Fernandez, F.; Jensen, M.; Runfeldt, M.; Shytle, R. D.; Tan, J. Green Tea Epigallocatechin-3-gallate (EGCG) Reduces β-Amyloid Mediated Cognitive Impairment and Modulates Tau Pathology in Alzheimer Transgenic Mice. *Brain Res.* **2008**, *1214*, 177−187.
(16) Bieschke, J.; Russ, J.; Friedrich, R. P.; Ehrnhoefer, D. E.; Wobst, H.; Neugebauer, K.; Wanker, E. E. EGCG Remodels Mature α-Synuclein and Amyloid-β Fibrils and Reduces Cellular Toxicity. *Proc. Natl. Acad. Sci. U.S.A.* **2010**, *107*, 7710−7715.
(17) Ferreira, N.; Cardoso, I.; Domingues, M. R.; Vitorino, R.; Bastos, M.; Bai, G.; Saraiva, M. J.; Almeida, M. R. Binding of Epigallocatechin-3-gallate to Transthyretin Modulates its Amyloidogenicity. *FEBS Lett.* **2009**, *583*, 3569−3576.
(18) Ehrnhoefer, D. E.; Duennwald, M.; Markovic, P.; Wacker, J. L.; Engemann, S.; Roark, M.; Legleiter, J.; Marsh, J. L.; Thompson, L. M.; Lindquist, S. Green Tea (−)-Epigallocatechin-gallate Modulates Early Events in Huntingtin Misfolding and Reduces Toxicity in Huntington's Disease Models. *Hum. Mol. Genet.* **2006**, *15*, 2743−2751.
(19) Ehrnhoefer, D. E.; Bieschke, J.; Boeddrich, A.; Herbst, M.; Masino, L.; Lurz, R.; Engemann, S.; Pastore, A.; Wanker, E. E. EGCG Redirects Amyloidogenic Polypeptides into Unstructured, Off-pathway Oligomers. *Nat. Struct. Mol. Biol.* **2008**, *15*, 558−566.
(20) Engel, M. F.; VandenAkker, C. C.; Schleeger, M.; Velikov, K. P.; Koenderink, G. H.; Bonn, M. The Polyphenol EGCG Inhibits Amyloid Formation Less Efficiently at Phospholipid Interfaces Than in Bulk Solution. *J. Am. Chem. Soc.* **2012**, *134*, 14781−14788.
(21) Hudson, S. A.; Ecroyd, H.; Dehle, F. C.; Musgrave, I. F.; Carver, J. A. (−)-Epigallocatechin-3-gallate (EGCG) Maintains κ-casein in its Pre-fibrillar State Without Redirecting its Aggregation Pathway. *J. Mol. Biol.* **2009**, *392*, 689−700.
(22) Palhano, F. L.; Lee, J.; Grimster, N. P.; Kelly, J. W. Toward the Molecular Mechanism(s) by Which EGCG Treatment Remodels Mature Amyloid Fibrils. *J. Am. Chem. Soc.* **2013**, *135*, 7503−7510.
(23) Siddiqui, I. A.; Mukhtar, H. Nanochemoprevention by Bioactive Food Components: a Perspective. *Pharm. Res.* **2010**, *27*, 1054−1060.
(24) Smith, A.; Giunta, B.; Bickford, P. C.; Fountain, M.; Tan, J.; Shytle, R. D. Nanolipidic Particles Improve the Bioavailability and α-secretase Inducing Ability of Epigallocatechin-3-gallate (EGCG) for the Treatment of Alzheimer's Disease. *Int. J. Pharm.* **2010**, *389*, 207−212.
(25) Dube, A.; Nicolazzo, J. A.; Larson, I. Chitosan Nanoparticles Enhance the Plasma Exposure of (−)-Epigallocatechin Gallate in Mice Through an Enhancement in Intestinal Stability. *Eur. J. Pharm. Sci.* **2011**, *44*, 422−426.
(26) Siddiqui, I. A.; Adhami, V. M.; Bharali, D. J.; Hafeez, B. B.; Asim, M.; Khwaja, S. I.; Ahmad, N.; Cui, H.; Mousa, S. A.; Mukhtar, H. Introducing Nanochemoprevention as a Novel Approach for Cancer Control: Proof of Principle with Green Tea Polyphenol Epigallocatechin-3-gallate. *Cancer Res.* **2009**, *69*, 1712−1716.
(27) Godoi, G. L.; de Oliveira Porciúncula, L.; Schulz, J. F.; Kaufmann, F. N.; da Rocha, J. B.; de Souza, D. O. G.; Ghisleni, G.; de Almeida, H. L., Jr. Selenium Compounds Prevent Amyloid β-Peptide Neurotoxicity in Rat Primary Hippocampal Neurons. *Neurochem. Res.* **2013**, *38*, 2359−2363.
(28) Kryukov, G. V.; Castellano, S.; Novoselov, S. V.; Lobanov, A. V.; Zehtab, O.; Guigó, R.; Gladyshev, V. N. Characterization of Mammalian Selenoproteomes. *Science* **2003**, *300*, 1439−1443.
(29) Bellinger, F.; Raman, A.; Reeves, M.; Berry, M. Regulation and Function of Selenoproteins in Human Disease. *Biochem. J.* **2009**, *422*, 11−22.
(30) Loef, M.; Schrauzer, G. N.; Walach, H. Selenium and Alzheimer's Disease: a Systematic Review. *J. Alzheimer's Dis.* **2011**, *26*, 81−104.
(31) Park, I. K.; Lasiene, J.; Chou, S. H.; Horner, P. J.; Pun, S. H. Neuron-Specific Delivery of Nucleic Acids Mediated by Tet1-modified Poly(Ethylenimine). *J. Gen. Intern. Med.* **2007**, *9*, 691−702.
(32) Liu, J. K.; Teng, Q.; Garrity-Moses, M.; Federici, T.; Tanase, D.; Imperiale, M. J.; Boulis, N. M. A novel Peptide Defined Through Phage Display for Therapeutic Protein and Vector Neuronal Targeting. *Neurobiol. Dis.* **2005**, *19*, 407−418.
(33) Mathew, A.; Fukuda, T.; Nagaoka, Y.; Hasumura, T.; Morimoto, H.; Yoshida, Y.; Maekawa, T.; Venugopal, K.; Kumar, D. S. Curcumin Loaded-PLGA Nanoparticles Conjugated with Tet-1 Peptide for Potential Use in Alzheimer's Disease. *PloS One* **2012**, *7*, e32616.
(34) Yu, H.; Ren, J.; Qu, X. Different Hydration Changes Accompanying Copper and Zinc Binding to Amyloid β-Peptide: Water Contribution to Metal Binding. *ChemBioChem* **2008**, *9*, 879−882.
(35) Song, Y.; Qu, K.; Xu, C.; Ren, J.; Qu, X. Visual and Quantitative Detection of Copper Ions Using Magnetic Silica Nanoparticles Clicked on Multiwalled Carbon Nanotubes. *Chem. Commun.* **2010**, *46*, 6572−6574.
(36) Geng, J.; Qu, K.; Ren, J.; Qu, X. Rapid and Efficient Screening of Alzheimer's Disease β-Amyloid Inhibitors Using Label-Free Gold Nanoparticles. *Mol. Biosyst.* **2010**, *6*, 2389−2391.
(37) Opazo, C.; Huang, X.; Cherny, R. A.; Moir, R. D.; Roher, A. E.; White, A. R.; Cappai, R.; Masters, C. L.; Tanzi, R. E.; Inestrosa, N. C. Metalloenzyme-Like Activity of Alzheimer's Disease β-Amyloid Cu-Dependent Catalytic Conversion of Dopamine, Cholesterol, and Biological Reducing Agents to Neurotoxic H_2O_2. *J. Biol. Chem.* **2002**, *277*, 40302−40308.
(38) Cimini, A.; D'Angelo, B.; Das, S.; Gentile, R.; Benedetti, E.; Singh, V.; Monaco, A. M.; Santucci, S.; Seal, S. Antibody-Conjugated PEGylated Cerium Oxide Nanoparticles for Specific Targeting of Aβ Aggregates Modulate Neuronal Survival Pathways. *Acta Biomater.* **2012**, *8*, 2056−2067.
(39) Liao, R.; Tang, Z.; Lei, Y.; Guo, B. Polyphenol-Reduced Graphene Oxide: Mechanism and Derivatization. *J. Phys. Chem. C* **2011**, *115*, 20740−20746.
(40) Soto, C. Protein Misfolding and Disease; Protein Refolding andTherapy. *FEBS Lett.* **2001**, *498*, 204−207.
(41) Biancalana, M.; Koide, S. Molecular Mechanism of Thioflavin-T Binding to Amyloid Fibrils. *Biochim. Biophys. Acta, Proteins Proteomics* **2010**, *1804*, 1405−1412.
(42) Jiang, T.; Zhi, X.-L.; Zhang, Y.-H.; Pan, L.-F.; Zhou, P. Inhibitory Effect of Curcumin on the Al (III)-induced Aβ< sub> 42</ sub> Aggregation and Neurotoxicity in Vitro. *Biochim. Biophys. Acta, Mol. Basis Dis.* **2012**, *1822*, 1207−1215.
(43) Levine, H.; Thioflavine, T. Interaction with Synthetic Alzheimer's Disease β-Amyloid Peptides: Detection of Amyloid Aggregation in Solution. *Protein Sci.* **1993**, *2*, 404−410.
(44) Lopez del Amo, J. M.; Fink, U.; Dasari, M.; Grelle, G.; Wanker, E. E.; Bieschke, J.; Reif, B. Structural Properties of EGCG-induced, Nontoxic Alzheimer's Disease Aβ Oligomers. *J. Mol. Biol.* **2012**, *421*, 517−524.
(45) Gupta, S.; Babu, P.; Surolia, A. Biphenyl Ethers Conjugated CdSe/ZnS Core/Shell Quantum Dots and Interpretation of the Mechanism of Amyloid Fibril Disruption. *Biomaterials* **2010**, *31*, 6809−6822.
(46) Saraiva, A. M.; Cardoso, I.; Saraiva, M. J.; Tauer, K.; Pereira, M. C.; Coelho, M. A.; Möhwald, H.; Brezesinski, G. Randomization of Amyloid-β-Peptide (1−42) Conformation by Sulfonated and Sulfated Nanoparticles Reduces Aggregation and Cytotoxicity. *Macromol. Biosci.* **2010**, *10*, 1152−1163.
(47) Pi, R.; Mao, X.; Chao, X.; Cheng, Z.; Liu, M.; Duan, X.; Ye, M.; Chen, X.; Mei, Z.; Liu, P. Tacrine-6-Ferulic Acid, a Novel Multifunctional Dimer, Inhibits Amyloid-β-Mediated Alzheimer's Disease-Associated Pathogenesis In Vitro and In Vivo. *PloS One* **2012**, *7*, e31921.
(48) Chonpathompikunlert, P.; Yoshitomi, T.; Han, J.; Isoda, H.; Nagasaki, Y. The Use of Nitroxide Radical-containing Nanoparticles Coupled with Piperine to Protect Neuroblastoma SH-SY5Y Cells from Aβ-induced Oxidative Stress. *Biomaterials* **2011**, *32*, 8605−8612.
(49) Omtri, R. S.; Davidson, M. W.; Arumugam, B.; Poduslo, J. F.; Kandimalla, K. K. Differences in the Cellular Uptake and Intracellular

Itineraries of Amyloid Beta Proteins 40 and 42: Ramifications for the Alzheimer's Drug Discovery. *Mol. Pharm.* **2012**, *9*, 1887−1897.